

Magnetic Optical Sensor Particles: A Flexible Analytical Tool for Microfluidics

Birgit Ungerböck,^a Siegfried Fellingner,^a Philipp Sulzer,^a Tobias Abel^a and Torsten Mayr^{*a}

^a Applied Sensors, Institute of Analytical Chemistry and Food Chemistry, Graz University of Technology, Stremayrgasse 9/3, 8010 Graz, Austria. Fax: +43 (0) 316 873 32502; Tel: +43 (0) 316 873 32504; E-mail: torsten.mayr@tugraz.at

Supporting information

S1

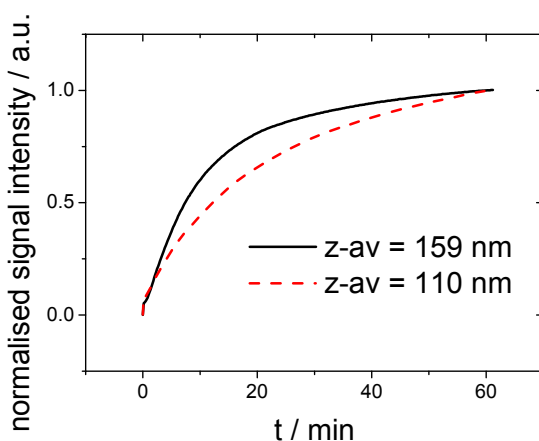


Fig. 1 Separation behavior of different particle sizes from a MOSeP dispersion. The graph illustrates observed signal intensities of MOSePs of varying particle diameters.

S2

Fig. 1 provides calibration data (Stern-Volmer plots) for four different oxygen sensing systems: (■) PtTpFPTBP (fiber optic read-out), (Δ) Ir(C_s)₂(acac) (lifetime imaging) (o) PtTFPP and MY (lifetime imaging) and (▼) PtTFPP and MY (RGB imaging). Table 1 summarizes characteristic calibration data, obtained by applying an adapted version of the two-site model of Demas et al.¹ for these sensing systems. Further information on sensor characterization can be found in previously published literature by Mistlberger et al.²

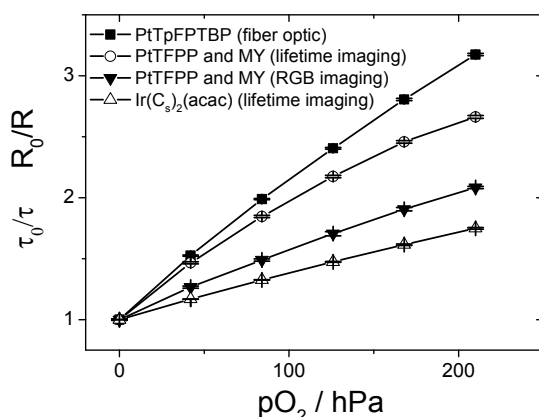


Fig. 2 Calibration plots for MOSePs applying four different oxygen sensing systems for oxygen monitoring from 0-100% air saturation: (■) PtTpFPTBP (fiber optic read-out), (Δ) Ir(C_s)₂(acac) (lifetime imaging) (o) PtTFPP and MY (lifetime imaging) and (▼) PtTFPP and MY (RGB imaging). The error bars show experimental data from 3 subsequent measurements.

S3

Table 1 Calibration data of luminescent magnetic nano sensor particles for fiber optic read-out and imaging applications for oxygen monitoring from 0-100% air saturation.

read-out	sensor dye ([(w/w)])	τ_0/τ / R_0/R_{air}	K_{SV} [hPa ⁻¹]	f_1
fiber optic	PtTpFPTBP (0.5)	3.17 ± 0.01	0.01408 ± 0.00018	0.916 ± 0.003
lifetime imaging	Ir(C ₆) ₂ (acac) (1.5)	1.75 ± 0.01	0.00486 ± 0.00002	0.847 ± 0.002
lifetime imaging	PtTFPP (1.5) and MY (3)	2.66 ± 0.01	0.01506 ± 0.00037	0.824 ± 0.006
RGB imaging	PtTFPP (1.5) and MY (3)	2.08 ± 0.01	0.00769 ± 0.00015	0.842 ± 0.008

S4

Computational Fluid Dynamics simulation studies using ANSYS CFX® software and Solid works revealed that the formed sensing spots do not cause turbulences. Figure 3 shows the velocity profile inside a microchannel with integrated magnetic sensor spots ($d = 2$ mm) for sensor spot heights of (A) $10 \mu\text{m}$ (realistic dimension) and (B) $200 \mu\text{m}$ (for comparison). A sensing spot with $10 \mu\text{m}$ spot height exhibited homogeneous velocity profiles across the whole microfluidic channel length and width with minimal variations of flow velocity. Computational Fluid Dynamics simulation studies showed that the flow runs around the sensor spot smoothly even for sensor spots with $200 \mu\text{m}$ height, although the simulation revealed inhomogeneous velocity profiles across the microfluidic channel length and width.

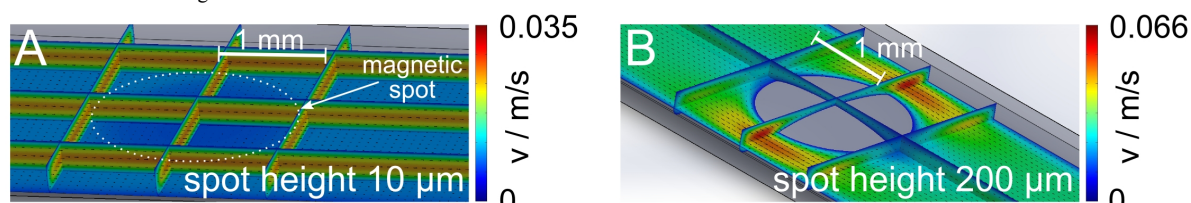


Fig. 3 Simulation results for flow and velocity profiles in microfluidic channels (height = $300 \mu\text{m}$, width = 3 mm) at a fluid flow of $1 \text{ mL}\cdot\text{min}^{-1}$ with integrated magnetic sensor spots ($d = 2 \text{ mm}$) for sensor spot heights of (A) $10 \mu\text{m}$ and (B) $200 \mu\text{m}$.

References

- 1 J. N. Demas, B. A. DeGraff, and W. Xu, *Anal. Chem.*, 1995, **67**, 1377–1380.
- 2 G. Mistlberger, K. Koren, E. Scheucher, D. Aigner, S. M. Borisov, A. Zankel, P. Pöhl, and I. Klimant, *Adv. Funct. Mater.*, 2010, **20**, 1842–1851.